Contribution from the Department of Chemistry,
The University of Kansas, Lawrence, Kansas 66045

Thermal Isomerization and Photoisomerization of a Chiral Chromium(III)–β-Diketone Complex in *n*-Hexane Solution

STEPHEN S. MINOR and GROVER W. EVERETT, Jr.*

Received December 16, 1975 AIC50904N

The four diastereomers of tris[(+)-3-acetylcamphorato]chromium(III) can be interconverted by photolysis in the ultraviolet or visible region with quantum yields of the order of 10^{-3} or by thermolysis at temperatures exceeding 100 °C. Quantum yields for formation of product isomers in *n*-hexane solution from individual starting isomers upon photolysis at 254, 350, and 577 nm are reported along with the corresponding rate constants for thermal isomerization at 134 °C. Analysis of selected ratios of rate constants and quantum yields indicate that, for cis isomers at least, both thermal isomerization and photoisomerization proceed primarily by a bond-breaking mechanism in which the intermediate or transition state has square-pyramidal coordination with the nonchelate ligand bound in the axial position.

Thermal isomerization rates of tris(β-diketonato)metal(III) complexes have been extensively investigated in recent years in attempts to establish the mechanisms involved.[1-8] Two distinct processes are generally held potentially responsible for intramolecular isomerization of these complexes. These are (1) twisting motions in which no metal–ligand bonds are broken and in which transition states result from rotation of ligands about real, pseudo, or imaginary threefold axes[9] and (2) processes in which one metal–ligand bond is broken, forming five-coordinate transition states. Idealized formulations of the latter are based on a square-pyramidal (SP) or trigonal-bipyramidal (TBP) coordination geometry, and several isomers are possible depending upon the location of the nonchelate ligand.

Despite efforts on numerous β-diketonate complexes, it has not yet been possible to establish the relative importance of the two basic mechanisms in solution.[10] Certain specific pathways can be excluded in some cases as the sole process, but no single pathway adequately explains the kinetic data.[4-6] Most evidence favors a combination of bond-breaking pathways.[5,6,8]

In contrast to the efforts in thermal isomerization kinetics, much less is known of the photochemically induced isomerization of this well-known class of complexes.[11] Indeed, relatively little information is available on the general photochemical behavior of β-diketonate complexes in solvents which are inert with respect to ligand substitution and redox processes.[11-13] Several tris(β-diketonato)chromium(III) complexes have been partially resolved using circularly polarized light,[14-17] and Stevenson has determined quantum yields for photoisomerization of tris(2,4-pentanedionato)-chromium(III) and tris(1,1,1-trifluoroacetylacetonato)chromium(III) in chlorobenzene solution.[14,17] Recent data for the latter complex indicate that geometrical isomerization and optical inversion occur upon irradiation of the ligand field band at 546 nm, and it was concluded that both bond rupture and twisting mechanisms are involved.[17] In an earlier study of the closely related complex tris(1,1,1-trifluoro-5,5-dimethyl-hexane-2,4-dionato)chromium(III) no geometrical isomerization was found upon irradiation of the d–d absorption band, but a photostationary state in which the isomer proportions are similar to those found upon thermal isomerization results from irradiation of the ligand bands.[18]

Detailed kinetic investigations of the complexes described above require at least partial resolution of enantiomeric species (Δ and Λ) in order to measure racemization rates. Resolution of electrically neutral complexes such as $(\beta\text{-dik})_3M^{III}$ (dik = diketonate) is difficult, but this problem can be completely avoided by using complexes of *chiral* β-diketonate ligands, such as I, where the ligand is (+)-3-acetylcamphor. Four stereoisomers (diastereomers) are possible for I; these are designated Δ-cis, Λ-cis, Δ-trans, and Λ-trans. They may be

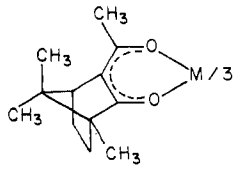

I

separated completely by silica gel chromatography for M^{3+} = Co^{3+}, Cr^{3+}, Rh^{3+}, and Ru^{3+}, and absolute configurations of all four diastereomers in each case are known.[19-21] Since for a given metal ion a pure diastereomer may isomerize thermally or photochemically to generate one or more of the remaining three, 12 processes are possible as shown in eq 1.

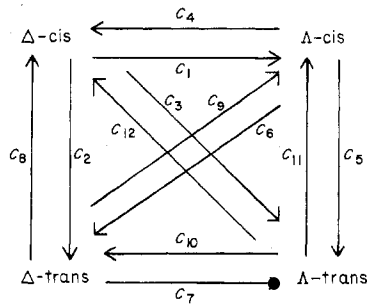

(1)

Here the 12 C_i's represent rate constants, k_i's, for thermal isomerization or quantum yields, ϕ_i's, for photoisomerization. Since some of these processes are excluded by certain isomerization mechanisms, determinations of the C_i's are expected to provide mechanistic information.

The present paper describes the kinetics of thermal isomerization of tris[(+)-3-acetylcamphorato]chromium(III), I, M = Cr^{3+}, hereafter abbreviated $Cr(atc)_3$. The quantum yields for photoisomerization as a function of wavelength are also presented, and a comparison of thermal and photochemical isomerization pathways is made.

Experimental Section

Materials. $Cr(atc)_3$ was prepared and separated into its four diastereomers as described previously.[19] Spectral grade *n*-hexane used for thermal isomerization and photoisomerization was dried by passage through a column of 4A molecular sieves and was stored in dry containers.

Thermal Isomerization. Rates of thermal isomerization of the four isomers of $Cr(atc)_3$ were measured using techniques developed earlier during a thermal isomerization study of $Ru(atc)_3$.[8] Solutions (6.3×10^{-3} M) of the individual disastereomers in *n*-hexane were sealed in capillary tubes and immersed in an oil bath at 134 °C. Tubes were removed at 15–30-min intervals, and 5–10 μl of the solutions was injected into the liquid chromatograph described below. Determination of the initial isomerization rates from chromatographic signal areas was carried out as described below and as described in a previous publication.[8]

The relative abundances of the diastereomers under equilibrium conditions were determined in a similar manner. Solutions of each diastereomer were heated at 134 °C until no further change in relative signal areas could be detected (~36 h). Relative equilibrium abundances thus obtained beginning with a given diastereomer were found to be in good agreement with those obtained from the other diastereomers.

Photoisomerization. Solutions of the individual diastereomers in dry, oxygen-free *n*-hexane were photolyzed at 254, 350, and 577 nm. Concentrations were 3.17×10^{-3} M (254 nm), 1.58×10^{-3} M (350 nm), and 3.17×10^{-3} M (577 nm). In the uv region these concentrations were such that essentially all of the light was captured in the 1-cm cell path. At 577 nm only 56% of the light was absorbed in the 2-cm cell path used; thus a correction for this was necessary in determining ϕ's. Photolysis in the uv region was carried out using a Rayonet RPR-100 reactor equipped with four RPR 3500-Å phosphor lamps (bandwidth 42 nm) or four RPR 2537-Å lamps (low-pressure mercury arc). The samples (10 ml) were contained in stoppered cylindrical quartz or Pyrex tubes held in a Rayonet MGR-100 Merry-Go-Round device. Aliquots (100 μl) were removed at regular intervals (10 min, 254 nm; 20 min, 350 nm) and injected into the liquid chromatograph. Mixing was accomplished by inverting the sample tubes just prior to removing aliquots. The concentrations of product isomers after each period of photolysis were determined from areas of their respective chromatographic signals as described below. Photolysis at 577 nm was accomplished using a Sargent-Welch 200-W superpressure mercury lamp and a 2-cm cylindrical sample cell. The lamp output was filtered by $CuCl_2$ and $K_2Cr_2O_7$ solutions which transmit light centered about 577 nm with a ~40-nm bandwidth.[22] Aliquots (5 μl) were removed from the sample cell at 20-min intervals and injected into the liquid chromatograph. Mixing was accomplished by inverting the cell several times prior to taking an aliquot.

A photostationary state was attained at each wavelength after extended photolysis: 254 nm, 4 lamps, 6 h; 350 nm, 16 lamps, 6 h; 577 nm, 30–50 h. At each wavelength relative isomer abundances obtained beginning with a given isomer were in good agreement with those obtained from the other isomers. Several unidentified chromatographic signals appeared during this period with photolysis at 254 nm and are attributed to decomposition products. However during the kinetic runs only signals arising from the four diastereomers of I were evident. Sample temperatures never exceeded 35 °C during photolysis. At this temperature no detectable thermal isomerization occurs during the time required to reach photostationary states.[23]

The light output of the lamps used at 254 and 350 nm was measured by routine ferric oxalate actinometry using the same experimental conditions as during photochemical isomerization. For the lamps and cylindrical cells used $I_a' = 2.40 \times 10^{-7}$ einstein/s at 254 nm and 1.61×10^{-7} einstein/s at 350 nm, where I_a' is the light *absorbed* per unit time using a specific cell.[24] The visible I_a' was measured using aqueous Reinecke salt[25] and was found to vary from 0.930×10^{-7} to 1.29×10^{-7} einstein/sec, depending upon the lamp used.

Attempts were made to carry out photoisomerization using the 200-W superpressure mercury lamp coupled with a Bausch and Lomb monochromator. However the light intensity proved far too small to effect photoisomerization within practical working time. For example, a 24-h photolysis in a 1-cm cell at 254 and 350 nm produced less than 2% of product isomers. Photoisomerization also occurs upon irradiation with a 70-mW He–Ne laser (633 nm) attached to a Raman spectrometer and with direct sunlight.

Chromatography. All high-pressure liquid chromatography was conducted on a Perkin-Elmer Series NF1210 liquid chromatograph with a NFLC-250 ultraviolet detector operating at 366 nm. The $Cr(atc)_3$ isomers were separated on a silica gel column (Corasil II) using a 15% (by volume) mixture of tetrahydrofuran in *n*-hexane at a flow rate of 0.4 ml/min. Retention times were 12 min for Δ-trans, 14 min for Λ-trans, 20 min for Λ-cis, and ~50 min for Δ-cis.

Treatment of Data. Preliminary work showed that the four diastereomers of $Cr(atc)_3$ give well-separated chromatographic signals under the above conditions. After thermal isomerization or photoisomerization of an initially pure isomer for a short period, the chromatogram of an aliquot shows a large signal for the initial isomer and one or more much smaller signals for product isomers. Relative areas of these signals, after correction for differences in ϵ_M values for the isomers at the wavelength of the detector, are equal to the relative isomer abundances. If it may be assumed[26] the only products of thermolysis or photolysis are the four diastereomers of $Cr(atc)_3$, the mole fraction of a given product isomer after time t is given by $A_p/\sum_i A_i$, where A's are corrected signal areas. In order to avoid secondary reactions during both photoisomerization and thermal kinetic runs, isomerization was allowed to proceed only until the combined signal areas of product isomers were about 20% of the signal area of the initial isomer. Since the original concentration of the initial isomer $[I_0]$ is known, the concentration of a product isomer at time t, $[P_t]$, is

$$[P_t] = \frac{A_p}{\sum_i A_i}[I_0] \tag{2}$$

First-order kinetics were assumed to hold for thermal isomerization of $Cr(atc)_3$, since this has been demonstrated for other tris(β-diketonate) complexes of Cr(III)[27] and other trivalent ions[4-6] in inert solvents. As discussed previously,[8] the simple rate expression describing formation of a product isomer

$$d[P]/dt = k_i[I] \tag{3}$$

may be integrated if [I] is assumed to remain constant for low conversion to products. The rate constants, k_i, may be determined from slopes of plots of $[P_t]/[I]$ vs. t. These plots are linear and pass through the origin for low conversion. Generally 10 data points were used in a least-squares evaluation of k.

Quantum yields for photoisomerization were determined in an analogous manner. The rate expression analogous to (3) is

$$d[P]/dt = \phi_i I_a'/V \tag{4}$$

where V is the cell volume in liters.[24] Integration of (4) and use of (2) give

$$\frac{A_p}{\sum_i A_i} = \frac{\phi_i I_a'}{[I_0]V}t \tag{5}$$

and quantum yields can be obtained from slopes of plots of $A_p/\sum_i A_i$ vs. t. Again, these plots are linear and pass through the origin, and least-squares treatment of 10 data points was carried out.

Chromatographic signal areas were obtained by planimetry.

Results and Discussion

Preliminary experiments demonstrated that both thermal isomerization and photoisomerization of $Cr(atc)_3$ are "clean"; that is, the only significant products are the diastereomers of $Cr(atc)_3$. Thermal isomerization occurs at temperatures in excess of 100 °C, and the temperature chosen for kinetic studies gives isomerization at convenient rates. Photoisomerization occurs at a variety of wavelengths, but quantum yields in all cases are low. As described in the Experimental Section, the light output of a high-pressure mercury lamp coupled with a monochromator proved far too low to effect isomerization at a useful rate. However the absorption bands of $Cr(atc)_3$ are rather broad, so the need for highly monochromatic light is not as severe as the need for a high photon flux. The absorption spectra of the four $Cr(atc)_3$ diastereomers are very similar and resemble that of tris(acetylacetonato)-chromium(III). The low-energy band in the visible region of the latter complex is assigned to the $^4A_{2g} \rightarrow {}^4T_{2g}$ transition in O_h symmetry,[28] but a theoretical treatment of the uv bands indicates extensive mixing of charge-transfer and ligand $\pi-\pi^*$ transitions.[29] The wavelengths chosen for the present investigation correspond to excitation of (1) the d–d band (570 nm), (2) a mixture of MLCT and $\pi-\pi^*$ transitions at 350 nm (the most intense absorption band above 240 nm), and (3) a region (254 nm) in which the predominant transition is believed[29] to be $\pi-\pi^*$.

High-pressure liquid chromatography proved to be a convenient method for determining relative isomer abundances at various stages of thermal isomerization and photoisomerization. Extremely small amounts ($\sim 10^{-8}$ mol) of an isomeric mixture give readily observed chromatographic signals using the 366-nm detector.

Table I. Quantum Yields and Thermal Rate Constants for Isomerization of $Cr(atc)_3$[a]

i	$10^3\phi_t$ (254 nm)	$10^3\phi_i$ (350 nm)	$10^3\phi_i$ (577 nm)	10^6k_i(134 °C), s^{-1}
1	3.0 ± 0.4	1.1 ± 0.2	0.76 ± 0.1	2.9 ± 0.6
2	8.3 ± 1	2.0 ± 0.3	1.0 ± 0.1	13.0 ± 0.8
3	6.3 ± 0.8	1.7 ± 0.2	0.47 ± 0.06	15.0 ± 0.4
4	3.5 ± 1[b]	0.55 ± 0.3[b]	0.88 ± 0.3[b]	2.6 ± 0.8[b]
5	5.9 ± 0.6	0.70 ± 0.06	0.43 ± 0.06	13.0 ± 1
6	13.0 ± 1	3.2 ± 0.4	4.7 ± 0.5	57.0 ± 2
7	8.0 ± 0.8	2.4 ± 0.3	1.2 ± 0.3	15.0 ± 0.7
8	1.5 ± 0.5[b]	0.31 ± 0.2[b]	0.21 ± 0.05[b]	3.8 ± 0.4[b]
9	2.2 ± 0.2	1.1 ± 0.1	0.60 ± 0.06	9.3 ± 0.5
10	9.8 ± 1	4.0 ± 0.4	3.5 ± 0.4	26.0 ± 1
11	0.88 ± 0.1	0.32 ± 0.04	0.13 ± 0.04[b]	4.2 ± 0.4
12	1.7 ± 0.5[b]	0.39 ± 0.2[b]	0.17 ± 0.04[b]	5.1 ± 0.4[b]

[a] Determined in *n*-hexane solution; ϕ_i and k_i where $i = 1$–12 are for the processes defined in eq 1. [b] Calculated using relative isomer abundances at equilibrium (see text).

Table II. Relative Abundances of $Cr(atc)_3$ Isomers at Photochemical and Thermal Equilibrium[a]

Isomer	% 254 nm	350 nm	577 nm	134 °C
Δ-cis	9.1 ± 1	7.2 ± 2	10.6 ± 0.9	11.9 ± 0.5
Λ-cis	7.7 ± 0.6	14.3 ± 1	9.1 ± 1	13.3 ± 0.2
Δ-trans	49.8 ± 2	46.8 ± 2	51.0 ± 1	41.0 ± 0.6
Λ-trans	33.4 ± 1	31.6 ± 0.4	29.3 ± 0.7	34.4 ± 0.6

[a] Error limits shown are average deviations from the mean of four values.

Errors in quantum yields and thermal rate constants are attributed primarily to uncertainties involved in actinometry and in measuring areas of small chromatographic signals and to errors inherent in the assumptions made in treating the data. These assumptions are (1) the concentration of the initial isomer remains unchanged at low conversion to products, (2) isomerization of the products is negligible, and (3) no products other than the isomers of $Cr(atc)_3$ are formed. Errors resulting from these three assumptions are not all determinate. With regard to assumption 3, no species other than isomers of $Cr(atc)_3$ could be detected by TLC, HPLC, or absorption spectroscopy. However, this does not rule out the presence of decomposition products with relatively low ϵ_M values or R_f values close to those of the isomers. Concerning assumption 2, it was pointed out earlier[8] that the observed k's and ϕ's could contain contributions from two- or three-step routes in eq 1 and they must be regarded as "apparent" k's and ϕ's. However significant product isomerization is expected to introduce curvature in the plots of $[P_t]/[I]$ and of $A_p/\sum_i A_i$ vs. t. This was not observed experimentally in any case. Isomerization in all cases was allowed to proceed only until the largest signal area of a product isomer was ~10% that of the starting isomer in hopes of avoiding problems connected with assumption 1 above.

Thermal Isomerization. Analysis of chromatographic signal areas at various times during thermolysis, as described in the Experimental Section, gives the 12 first-order rate constants $k_i \equiv C_i$ as defined in eq 1. These are given in Table I. Due to inaccuracies in measuring the area of the weak, broad signal arising from the Δ-cis isomer, rate constants k_4, k_8, and k_{12} were calculated using the appropriate relative isomer abundances under equilibrium conditions (Table II) and rate constants k_1, k_2, and k_3, respectively. Error limits shown for the rate constants in Table I represent the averages of deviations of $[P_t]/[I]t$ from the slopes of the least-squares lines in plots of $[P_t]/[I]$ vs. t except for k_4, k_8, and k_{12}, where errors in relative isomer abundances at equilibrium are also included.

In order to facilitate analysis of these rate constants in deducing the mechanism(s) of isomerization, Table III was constructed. Selected ratios of rate constants expected for several plausible mechanistic pathways were determined from statistical considerations.[6,8] The assumptions were made that (1) for bond-breaking mechanisms, any Cr–O bond may be broken with equal probability in forming the transition state and (2) no stereoselective effects are operative during formation of products from the transition state. In Table III, columns 1 and 4 give the ratios of the statistically expected rates of formation of inversion (Δ ⇌ Λ) products to the overall rates of formation of rearrangement (cis ⇌ trans) products. Columns 2 and 5 give the ratios of the rate of inversion without rearrangement to the rates of all other processes, and columns 3 and 6 give the ratio of the rate of rearrangement without inversion to the rates of all other processes. Experimental values of these ratios are presented in Table IV.

All twist mechanisms require at least one k to be zero for each diastereomer; thus twist mechanisms a–c (Table III) cannot be solely responsible for the thermal isomerization of $Cr(atc)_3$. For example, beginning with the Δ-cis isomer a trigonal twist mechanism would require $k_1 \neq 0$ but $k_2 = k_3 = 0$. Therefore bond-breaking mechanisms appear to play a dominant role in the thermal isomerization of $Cr(atc)_3$. Two k's must be zero in each case if isomerization occurs solely through a TBP transition state (or intermediate) with the nonchelate ligand in an equatorial position (mechanism d). At least one k must be zero for TBP (axial) and SP (basal) transition states, which are kinetically indistinguishable[6] (mechanism e).

The best fit of statistical and experimental data for a single mechanism occurs with mechanism i for Δ-cis and Δ-trans isomers. This involves a square-pyramidal transition state with a nonchelate ligand bound axially and assumes equal probability of "primary" and "secondary" torsional motions[6] of

Table III. Statistical Ratios of Quantum Yields and Thermal Rate Constants for Various Isomerization Mechanisms[a]

Mechanism or transition state	Cis isomers[b] $(C_1 + C_3)/(C_2 + C_3)$ or $(C_4 + C_6)/(C_5 + C_6)$	$C_1/(C_2 + C_3)$ or $C_4/(C_5 + C_6)$	$C_2/(C_1 + C_3)$ or $C_5/(C_4 + C_6)$	Trans isomers[b] $(C_7 + C_9)/(C_8 + C_9)$ or $(C_{10} + C_{12})/(C_{11} + C_{12})$	$C_7/C_8 + C_9)$ or $C_{10}/(C_{11} + C_{12})$	$C_8/C_7 + C_9)$ or $C_{11}/(C_{10} + C_{12})$
(a) trigonal twist	∞	∞	0	∞	∞	0
(b) rhombic twist	1	0	0	3	2	0
(c) combined twist[c]	1.33	0.33	0	4	3	0
(d) TBP equatorial	0	0	∞	0	0	∞
(e) TBP axial, SP basal	1	0	0	3	2	0
(f) combined TBP[c]	0.5	0	1	1.5	1	0.33
(g) SP axial primary process	1	0.5	0.5	3	2.5	0.17
(h) SP axial secondary process	1	0	0	3	2	0
(i) SP axial combined processes[c]	0.67	0.08	0.62	2	1.4	0.21

[a] See text for assumptions made in constructing this table. [b] The symbol C represents ϕ for photoisomerization or k for thermal isomerization as defined in eq 1. [c] Combined mechanisms assume equal probability of their components.

Table IV. Experimental Ratios of Quantum Yields and Thermal Rate Constants for $Cr(atc)_3$

	Cis isomers[a]			Trans isomers[a]		
	$(C_1 + C_3)/(C_2 + C_3)$ or $(C_4 + C_6)/(C_5 + C_6)$	$C_1/(C_2 + C_3)$ or $C_4/(C_5 + C_6)$	$C_2/(C_1 + C_3)$ or $C_5/(C_4 + C_6)$	$(C_7 + C_9)/(C_8 + C_9)$ or $(C_{10} + C_{12})/(C_{11} + C_{12})$	$C_7/(C_8 + C_9)$ or $C_{10}/(C_{11} + C_{12})$	$C_8/(C_7 + C_9)$ or $C_{11}/(C_{10} + C_{12})$
			Thermal Isomerization, 134 °C			
Δ isomers	0.64 ± 0.06	0.10 ± 0.02	0.75 ± 0.09	1.9 ± 0.2	1.2 ± 0.1	0.15 ± 0.02
Λ isomers	0.85 ± 0.08	0.04 ± 0.01	0.22 ± 0.03	3.3 ± 0.4	2.8 ± 0.3	0.14 ± 0.02
			Photochemical Isomerization, 254 nm			
Δ isomers	0.64 ± 0.2	0.22 ± 0.05	0.89 ± 0.2	2.8 ± 0.8	2.2 ± 0.6	0.15 ± 0.06
Λ isomers	0.87 ± 0.2	0.19 ± 0.08	0.36 ± 0.08	4.5 ± 2	3.8 ± 1	0.08 ± 0.02
			Photochemical Isomerization, 350 nm			
Δ isomers	0.76 ± 0.2	0.32 ± 0.08	0.69 ± 0.2	2.6 ± 0.8	1.8 ± 0.6	0.08 ± 0.05
Λ isomers	0.96 ± 0.3	0.15 ± 0.1	0.18 ± 0.05	6.7 ± 3	6.2 ± 3	0.07 ± 0.02
			Photochemical Isomerization, 577 nm			
Δ isomers	0.84 ± 0.2	0.52 ± 0.1	0.81 ± 0.2	2.2 ± 0.7	1.5 ± 0.5	0.12 ± 0.05
Λ isomers	1.1 ± 0.3	0.17 ± 0.08	0.08 ± 0.02	12.2 ± 5	11.7 ± 4	0.04 ± 0.02

[a] The symbol C represents ϕ for photoisomerization or k for thermal isomerization as defined in eq 1.

the other ligands in formation of both the transition state and the products. Results for the Λ-trans isomer seem to favor mechanism g, which involves an SP axial transition state and a predominance of the "primary" process. The experimental data for the Λ-cis isomer do not closely match statistical results for any single mechanism in Table III. However, statistical data for an SP axial transition state which assumes a predominance of the secondary process (but not excluding the primary process) are in fair agreement with the experimental results.[30]

In summary, the thermal data indicate a predominance of bond-breaking processes involving SP axial transition states. Small contributions from other processes cannot be excluded, however. A more satisfactory match of statistical and experimental data would likely be possible using weighted combinations of several mechanisms, but the accuracy of the data and the assumptions made during statistical analysis of the data do not justify this.

Photoisomerization. Quantum yields for photoisomerization of $Cr(atc)_3$ at 254, 350, and 577 nm are listed in Table I. They are of the same order of magnitude as previously reported quantum yields for photoisomerization of chromium(III)–β-diketonate complexes.[14,17,18] As was the case for thermal isomerization, chromatographic signal areas for the Δ-cis isomer were always weak and broad, so ϕ_4, ϕ_8, and ϕ_{12} were determined from measured values of ϕ_1, ϕ_2, and ϕ_3 and the appropriate ratios of isomer abundances in the photostationary state at each wavelength. This was also done for ϕ_{11} at 577 nm. The 12 ϕ's determined at each wavelength can, in principle, be used to infer mechanistic information in exactly the same manner as was done for the thermal isomerization rate constants. Thus the statistical ratios of rate constants determined for various mechanisms in Table III apply also to corresponding ratios of ϕ's. These may be compared with the experimental ratios of ϕ's at each wavelength, given in Table IV.

Errors shown for photochemical data in Tables I and IV are larger than those for thermal data since errors in actinometry combine with deviations from the slopes of the least-squares lines in plots of $A_p/\sum_i A_i$ vs. time and, in the cases mentioned above, with errors in the relative isomer abundances in the photostationary state. Table IV reveals a rough similarity among the experimental data for thermal isomerization and photoisomerization at all three wavelengths for each cis isomer. For the Δ-cis isomer, the data at 254 nm most closely match the statistical values for mechanism i. The trend toward larger deviation from statistical values for mechanism i with increasing wavelength for Δ-cis can be accounted for by assuming a larger contribution from the primary process in an SP axial transition state.[30]

For the Λ-cis isomer the agreement among experimental ratios for thermal isomerization and photoisomerization is better than the agreement with any single set of statistical values in Table III. However, it appears than bond-breaking processes with SP transition states predominate at each wavelength, since appreciable contributions from other mechanisms having 0 or ∞ ratios would not result in the observed ratios. The observed ratios can be accounted for, roughly, by assuming a larger contribution from the secondary process with an SP axial transition state,[30] but small contributions from other mechanisms cannot be excluded.

For the Δ-trans isomer no ϕ was found to be zero; thus the data indicate a bond-breaking process occurring at all wavelengths. The best fit of experimental and statistical data assumes an SP axial transition state or intermediate.

Data for the Λ-trans isomer are less readily interpreted. The agreement between thermal and photochemical data at all wavelengths is poor, and experimental quantum yield ratios cannot be fit even approximately to any of the statistical values. It cannot be ascertained whether the apparent trend (especially for 577 nm) of experimental ratios toward the statistical values for mechanism a is real. Although the four species here are diastereomers and could isomerize by different processes, it is unlikely that the processes will differ greatly. Bond-breaking processes appear to dominate at all wavelengths for the other three isomers; thus an unusually large contribution from a trigonal twist process is not expected for Λ-trans. Possibly the statistical ϕ ratios are misleading here since they do not take into account intramolecular steric interactions which could favor one mechanism over another. There are six nonequivalent bonds for trans isomers (C_1 symmetry) compared to two for cis isomers (C_3). Thus the assumptions of equal probability of any bond breaking to form the transition state and equal probability of reattack at any available position to form products are not so likely to be valid for the trans isomers; i.e., a stereoselective effect may be important. It is not clear, however, why these effects are apparently small for the Δ-trans isomer.

Summary and Conclusions

Error limits shown in Tables I and IV for thermal rate constants and photochemical quantum yields are believed to be realistic determinate errors. As discussed above, indeterminate errors also exist and can be demonstrated by comparing ratios of ϕ's or k's, connecting two isomers, with the corresponding ratios of the isomer abundances at equilibrium (in cases where this relationship was not used to

determine a value of ϕ or k). In three cases the discrepancy is well outside the limits of determinate error. The largest discrepancy occurs for Δ-trans ⇌ Λ-cis during thermal isomerization where $k_9/k_6 = 0.16$ and $[\Lambda\text{-cis}]_{eq}/[\Delta\text{-trans}]_{eq} = 0.32$. Thus the data presented here should not be used for detailed mechanistic arguments in which various mechanisms a–i are assigned fractional contributions to the overall isomerization. However, the ϕ's and k's are believed to be sufficiently accurate that appropriately selected ratios of these quantities may be used *qualitatively* to deduce the general type of mechanism involved in isomerization.

The experimental data presented here, at least for cis isomers, show a parallel between thermal rate constant ratios and corresponding ratios of photochemical quantum yields at each wavelength. The implication is that thermal and photochemical isomerizations of Δ- and Λ-*cis*-$Cr(atc)_3$ proceed via a common mechanism. Unfortunately, the data for trans isomers are less readily interpreted.

A number of mechanisms can be eliminated as the sole isomerization mechanism in each case, and, with the exception of the Λ-trans isomer for which no further conclusions can be drawn, the data strongly suggest both thermal isomerization and photoisomerization proceed by bond rupture to form an SP axial complex as the predominant intermediate or transition state.[31] Here light probably serves to break a Cr–O bond, a process which occurs thermally to a measurable extent only above 100 °C. In both cases formation of products from the transition state or intermediate proceeds in a similar manner.

The quantum yields shown in Table I for 577 and 350 nm show a rough parallel in magnitude for most values of *i*. Somewhat larger values are found at 254 nm, but the general trends in relative magnitude are qualitatively the same. This may indicate that a common excited state is involved in bond breaking, at least upon irradiation at 350 and 577 nm. This excited state is likely to be one closely related[32] to the $^4T_{2g}$ state in complexes having O_h symmetry, since appreciable Cr–O bond distortions are expected. Upper excited states resulting from irradiation at 350 nm (and possibly also at 254 nm) are probably rapidly deactivated to this reactive excited state.

Acknowledgment. This research was supported by the Research Corp., the University of Kansas General Research Fund, and Biomedical Sciences Support Grant RR-07037. We are indebted to Professor Richard Givens for advice and helpful discussions.

Registry No. $Cr(atc)_3$, 42539-33-3; Δ-*cis*-$Cr(atc)_3$, 32490-78-1; Λ-*cis*-$Cr(atc)_3$, 31116-46-8; Δ-*trans*-$Cr(atc)_3$, 32490-76-9; Λ-*trans*-$Cr(atc)_3$, 32592-78-2.

References and Notes

(1) F. Basolo and R. G. Pearson, "Mechanisms of Inorganic Reactions", 2d ed, Wiley, New York, N.Y., 1967, Chapter 4.
(2) J. J. Fortman and R. E. Sievers, *Coord. Chem. Rev.*, **6**, 331 (1971).
(3) N. Serpone and D. G. Bickley, *Prog. Inorg. Chem.*, **17**, 391 (1972).
(4) J. R. Hutchison, J. G. Gordon, II, and R. H. Holm, *Inorg. Chem.*, **10**, 1004 (1971).
(5) A. Y. Girgis and R. C. Fay, *J. Am. Chem. Soc.*, **92**, 7061 (1970).
(6) J. G. Gordon, II, and R. H. Holm, *J. Am. Chem. Soc.*, **92**, 5319 (1970).
(7) C. Kutal and R. E. Sievers, *Inorg. Chem.*, **13**, 897 (1974).
(8) G. W. Everett, Jr., and R. R. Horn, *J. Am. Chem. Soc.*, **96**, 2087 (1974).
(9) C. S. Springer, Jr., and R. E. Sievers, *Inorg. Chem.*, **6**, 852 (1967).
(10) In a recent study of the isomerization kinetics of tris(1,1,1-trifluoro-2,4-pentanedionato)chromium(III) in the gas phase, it was proposed that a twist mechanism is the most likely pathway from a comparison of the gas-phase activation energy of isomerization and the Cr–O bond energy.[7]
(11) R. L. Lintvedt in "Concepts in Photochemistry", A. Adamson and P. D. Fleischauer, Ed., Wiley, New York, N.Y., 1975.
(12) W. L. Waltz and R. G. Sutherland, *Chem. Soc. Rev.*, **1**, 241 (1972).
(13) V. Balzani and V. Carassiti, "Photochemistry of Coordination Compounds", Academic Press, New York, N.Y., 1970.
(14) K. L. Stevenson, *J. Am. Chem. Soc.*, **94**, 6652 (1972).
(15) H. Yoneda, Y. Nakashima, and U. Sakaguchi, *Chem. Lett.*, 1343 (1973).
(16) K. L. Stevenson, Abstracts, 168th National Meeting of the American Chemical Society, Atlantic City, N.J., Sept 1974, No. INOR 142.
(17) K. L. Stevenson and T. P. vanden Driesche, *J. Am. Chem. Soc.*, **96**, 7964 (1974).
(18) R. D. Koob, J. Beusen, S. Anderson, D. Gerger, S. P. Pappas, and M. L. Morris, *J. Chem. Soc., Chem. Commun.*, 966 (1972).
(19) R. M. King and G. W. Everett, Jr., *Inorg. Chem.*, **10**, 1237 (1971).
(20) G. W. Everett, Jr., and R. M. King, *Inorg. Chem.*, **11**, 2041 (1972).
(21) G. W. Everett, Jr., and A. Johnson, *Inorg. Chem.*, **13**, 489 (1974).
(22) J. G. Calvert and J. N. Pitts, "Photochemistry", Wiley, New York, N.Y., 1966, pp 740–741.
(23) Thermal isomerization is negligible even at 100 °C over a 24-h period.
(24) See ref 13, Chapter 2.
(25) E. E. Wegner and A. W. Adamson, *J. Am. Chem. Soc.*, **88**, 394 (1966).
(26) This assumption is supported by the fact that uv and visible absorption spectra of the isomeric mixtures after low-conversion photolysis or thermolysis are essentially identical with spectra obtained on samples prepared by mixing pure isomers prior to photolysis or thermolysis.
(27) R. C. Fay, A. Y. Girgis, and U. Klabunde, *J. Am. Chem. Soc.*, **92**, 7056 (1970).
(28) D. W. Barnum, *J. Inorg. Nucl. Chem.*, **21**, 221 (1961).
(29) I. Hanazaki, F. Hanazaki, and S. Nagakura, *J. Chem. Phys.*, **50**, 276 (1969).
(30) Note that statistical ratios of k's or ϕ's for combined processes in Table III are not simple weighted averages of ratios for the component mechanisms. For example, assuming a 10:1 ratio of primary to secondary processes and an SP axial transition state, the ratios appropriate to columns 1, 2, and 3 of Table III are 0.77, 0.26, and 0.63, respectively. Assuming a 1:4 ratio of primary to secondary processes, these ratios become 0.76, 0.02, and 0.34, respectively, and assuming a 1:10 ratio of primary to secondary processes, these ratios are 0.86, <0.01, and 0.17, respectively.
(31) Although both steric and electronic effects must play a role in determining the transition-state stereochemistry, it is perhaps significant to point out that SP transition states are considerably more favorable than TBP transition states from crystal field energy calculations.
(32) The cis isomers of $Cr(atc)_3$ have only C_3 symmetry in the ground state, and the $^4T_{2g}$ (O_h) state is split into two components (^4A and ^4E). This splitting is not apparent in the absorption spectra, but it can readily be seen in CD spectra.[19]